# Journal Pre-proof

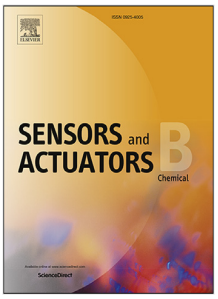


A combined experimental and DFT study on the zero valent iron/reduced graphene oxide doped QCM sensor for determination of trace concentrations of As using a Flow-batch system

Julián Gutiérrez, Yael N. Robein, Julián Juan, María S. Di Nezio, Carolina Pistonesi, Estela A. González, Rodrigo Santos, Marcelo F. Pistonesi

PII: S0925-4005(23)01951-2
DOI: https://doi.org/10.1016/j.snb.2023.135233
Reference: SNB 135233

To appear in: *Sensors and Actuators: B. Chemical*

Received date : 7 September 2023
Revised date : 22 December 2023
Accepted date : 23 December 2023

Please cite this article as: J. Gutiérrez, Y.N. Robein, J. Juan et al., A combined experimental and DFT study on the zero valent iron/reduced graphene oxide doped QCM sensor for determination of trace concentrations of As using a Flow-batch system, *Sensors and Actuators: B. Chemical* (2023), doi: https://doi.org/10.1016/j.snb.2023.135233.

# A combined experimental and DFT study on the zero valent iron/reduced graphene oxide doped QCM sensor for determination of trace concentrations of As using a Flow-batch system.

Julián Gutiérrez[a], Yael N. Robein[c], Julian Juan[b], María S. Di Nezio[c], Carolina Pistonesi[b], Estela A. González[b], Rodrigo Santos[a], Marcelo F. Pistonesi[c,d]

[a]*Dep. Ing. Eléctrica y Computadoras, Universidad Nacional del Sur, ICIC (UNS-CONICET), Bahía Blanca, 8000, Buenos Aires, Argentina*
[b]*Departamento de Física, Universidad Nacional del Sur, IFISUR (UNS-CONICET), Bahía Blanca, 8000, Buenos Aires, Argentina*
[c]*Departamento de Química, Universidad Nacional del Sur, INQUISUR (UNS-CONICET), Bahía Blanca, 8000, Buenos Aires, Argentina*
[d]*Comisión de Investigaciones Científicas Prov. Buenos Aires, Argentina*

**Abstract**

A sensor based on a gold Quartz Crystal Microbalance (QCM) modified with nanoscale zero-valent iron nanoparticles (nZVI) anchored to reduced graphene oxide (rGO) was developed. An automated measurement microsystem was employed using QCM (modified and unmodified) as an arsine detector device. The QCM measurements of frequency changes are associated with total As concentration (III/V) in the samples. The gold surface QCM modification with nZVI/rGO improved the sensitivity in total As determination. The limit of detection (LOD) was 0.0062 $ng\ mL^{-1}$ for QCM-Au/nZVI/rGO, 100 times higher than the unmodified QCM-Au sensor. Moreover, studies of adsorption energy and electron density of As with QCM-Au/nZVI/rGO and QCM-Au systems were performed. For this purpose, Density Functional Theory (DFT) methodology was used employing arsine adsorption on magnetite nanoparticles supported on graphene, and also on Au as models. This theoretical-experimental research allows us to acquire knowledge of the interaction of Au/nZVI/rGO with As and confirms the experimental results.

*Keywords:* Arsenic determination, DFT, Nanoparticles nZVI/rGO,

Quartz Crystal Microbalance Sensor, Flow-batch
*PACS:* 0000, 1111
*2000 MSC:* 0000, 1111

## 1. Introduction

Quartz crystal microbalance (QCM)-based sensors are widely used in various fields such as chemistry, biochemistry, and environmental sciences for trace analysis [1]. The QCM is a piezoelectric gravimetric sensor, i.e., it detects small mass changes in the nanogram range on its surface. It works by transducing mass changes into variations of its resonance frequency [2]. This device can be used in analytical systems to analyze liquid or gaseous samples in real-time and with the possibility of dissipation measurement (QCM-D) depending on the methodology used [3]. In recent times, the use of these sensors has increased due to high sensitivity, robustness, and small-size design that facilitates the integration into automated systems for routine analysis [4, 5]. Although they present good analytical responses, it is possible to improve the performance in terms of sensitivity and selectivity by doping the piezoelectric surface with different components (organic and inorganic) [6]. For example, the coating of the sensor surface with nanoparticles has been recently proposed for the determination of pollutants, such as heavy metals [7]. These nanomaterials increase the effective surface area of the electrode, allowing it to enhance the interaction/adsorption of the analytes. Various types of nanomaterials based on iron nanoparticles have recently been used to remove arsenic (As) from water of industrial and agricultural origin. The determination of As is of major interest for public health policies as there are several millions of people who suffer the consequences of consuming contaminated water without knowing it [8].

Several Iron-based materials with low cost have proven to be knowledgeable for the removal of As such as iron oxide, zero-valent iron and others [9, 10, 11]. Among iron-based materials, nanoscale zero valence iron (nZVI) particles have gained much importance in remediation studies related to As adsorption in natural waters. The nZVI have been shown to have an important interaction with As and promote a reduction reaction on its surface, allowing its capture. However, to have better stability and immobilize these nanoparticles, a support is required [12, 13, 14]. As a support candidate, the reduced graphene oxide (rGO), has several advantageous aspects such as large specific surface area, structural and electrochemical properties. Moreover, it is a favorable system for nZVI immobilization [15, 16].

The combination of the nZVI and rGO, known as the nZVI/rGO system, is interesting and proven to be a better candidate than isolated nZVI, for the removal of pollutants, as shown by experimental and theoretical studies [17, 18]. Wang et al. have confirmed with studies in batch the adsorption of arsenic by materials of zero-valent iron nanoparticles (nZVI) anchored to reduced graphene oxide (rGO) in water compared to bare nZVI [19].

From a theoretical-experiment perspective, it is common to come across studies that analyze the interaction of the sensor surface with the modified substrate or with the analyte to be determined [20]. This type of study allows for evaluating the feasibility of its development. Density Functional Theory (DFT) provides a well-established methodology for modeling molecular and atomic systems in terms of reactions and adsorption, among other topics. For example, one of the areas to which it is applicable is the determination of contaminants, regardless of the aggregation state in which you work, presenting itself as a valuable tool [21, 22]. For instance, Arivarasi Arularasan et al. evaluated the adsorption capacity of heavy metals for water quality analysis using DFT [23]. In the case of As, interactions with certain metallic nanocomposites have been studied, with those composed of iron being among the most promising [24, 25]. Leslie L. Alfonso Tobón et al. sought to predict the adsorption capacity of iron-based nanomaterials with metallic impurities for arsenic removal [26]. In addition to these, a significant amount of research has shown that carbon-based nanocomposites, such as graphene, also demonstrate a high adsorption capacity for these types of contaminant [27, 28]. In our group, Vinicius de Lima et al. modeled zero-valent iron molecules supported on reduced graphene oxide, aiming to leverage the properties of both materials. Once this was done, the interaction with arsenic was evaluated for its determination in water samples [18].

In this work, we developed a gold QCM sensor based on zero-valent iron nanoparticles (nZVI) supported on reduced graphene oxide (rGO) sheets for the determination of total As in water samples. The determination of this contaminant is related to the quantity of arsine ($AsH_3$) generated by a Flow-batch system from As solutions adsorbed onto the QCM sensor. The performance of this sensor was compared with the sensor without nanoparticles. Additionally, DFT was used to analyze the interactions of small-sized magnetite ($Fe_3O_4$) and graphene clusters to model the nZVI/rGO substrate, as well as gold sheets and $AsH_3$ molecules to simulate the sensor surface and analyte, respectively. In order to corroborate the results of these experi-

mental systems, DFT calculations can provide an interesting perspective to verify and contribute new ideas for future experimental work. Regarding the subject of study of this work, we have not found a theoretical work of arsine adsorption employing a QCM sensor coated with these nanoparticles.

This article reports the theoretical and experimental study to demonstrate that this prototype could be used in the determination of arsenic in natural water samples in comparison with reference methodologies that are expensive, complex analysis processes and require qualified personnel [29, 30, 31, 32].

## 2. Material and methods

### *2.1. Experimental section*

#### *2.1.1. Reagents and solutions*

The reagents were of analytical grade, and the solutions were prepared using ultra-pure water (18 MΩ). A stock solution of 1.0 $mg\ mL^{-1}$ of As(III) was prepared dissolving the required amount of $As_2O_3$ (Cica-Merck) in water. Standard solution 10 $ng\ mL^{-1}$ was obtained from a dilution of the stock solution, and from this, the As test solutions were prepared to carry out the studies. A 1.0% $(m/v)$ $NaBH_4$ solution was used as a reducing agent. For this proposal, 0.5 $g$ of $NaBH_4$ (Biopack) was dissolved in 5.0 $mL$ of 0.1% NaOH (Anedra). 2.0 M HCl solution (Cicarelli) was used to adjust the pH.

#### *2.1.2. Flow-batch system*

In this work, a modification of the Flow-batch system described by Gutierrez et al. was used for the determination of total As [33] (see Figure 1a). In order to decrease amounts of reagents and optimize the system's connections, two chambers were designed. The first one is a homemade four-channel reaction chamber (RC), which schematic view is presented in Figure 1b. The RC is built with Teflon due is an inert and durable material that has the advantage of being easy to clean, ensuring no cross-contamination between assays.

Moreover, the sensing chamber (SC, Figure 1c-1d) was designed in the laboratory and built using a 3D printer (HellBot, model Magna 2 300). The SC consists of two pieces (top and bottom), which couple the QCM with two O-rings and joined by a thread. The upper part of the chamber was designed with two channels to insert pump tubes in order to allow the passage of fluids (0.508 mm internal diameter). The bottom piece was

designed for the electronics connections, where it has a PCB (Printed Circuit Board) with gold pins to make electrical contact with the crystal.

The reaction to obtain arsine ($AsH_3$) from As (III and/or V) present in aqueous medium depends on the pH of the medium. In our case, the determination of total As must be carried out by first oxidizing As(III) to As(V) (using HCl), and then reducing all As(V) to the hydride by using a reducing solution, such as $NaBH_4$, in an alkaline medium (Equations 1-2) [34].

$$H_3AsO_4 + BH_4^- + H^+ -> H_3AsO_3 + H_2O + BH_3 \quad (1)$$

$$H_3AsO_3 + 3BH_4^- + 3H^+ -> AsH_3 + 3BH_3 + 3H_2O \quad (2)$$

The Flow-batch system was presented as a promising tool to carry out the quantification of total As, but as in the implementation of other chemical application systems, it is of vital importance to ensure the optimization of the variables that affect the reliability of the results. For this particular case, the variables of reaction pH, reagent concentration and pump geometry conditions are the ones that stand out. For example, pH and reagent concentration can influence reaction speed, selectivity and accuracy of total As quantification. And on the other hand, the geometrical characteristics of the pump can affect the pump efficiency, among other things. For this reason, we used the values already optimized in Vallese et. al. [35] for the development of the work in order to obtain reproducible and accurate results.

*2.1.3. Flow-batch procedure*

Initially, before starting the measurements, the As test solution, $NaBH_4$ and HCl solution were pumped and recirculated into the system. Then, the solenoid valves V1, V2 and V3 are switched on for 10 s to load the channels. Hence, 15 $mL$ of the test solutions and 100 $\mu L$ HCl were introduced into RC for 360 s employing V1 and V3. Therefore, the peristaltic pump (PP) was turned off for 120 s while magnetic stirring (MS) was switched on and the impedance analyzer was initialized to obtain an initial signal. In the next step, the PP and V2 were turned on and 1.8 $mL$ $NaBH_4$ 1.0% $m/v$ solution was introduced for 150 s into the RC to promote the release of arsine. Then, the PP was switched off and the measurement was continued for 300 s to stabilize the signal. Finally, data logging was stopped, MS was switched

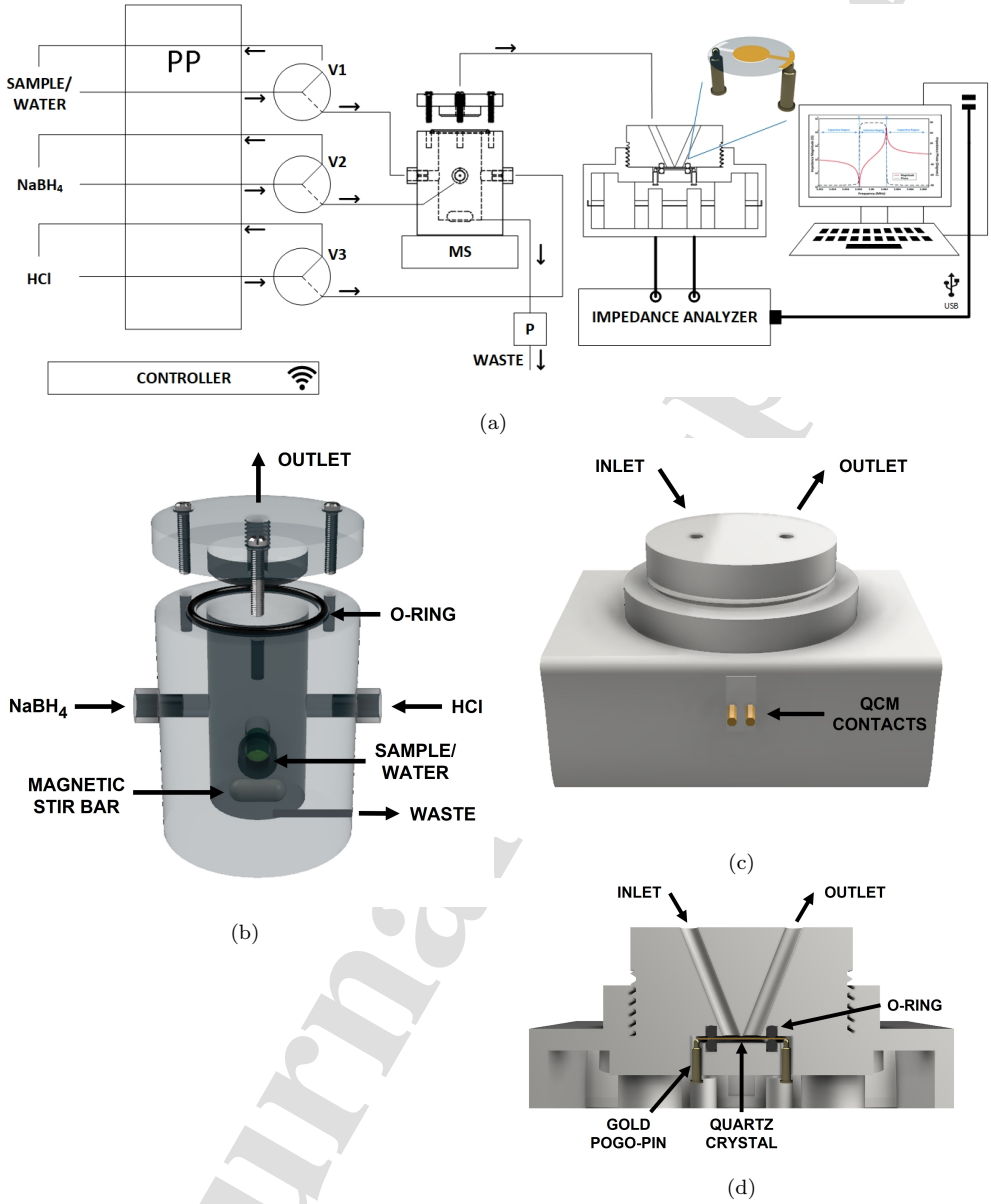


Figure 1: a) Schematic diagram of the Flow-batch system for the determination of arsenic, b) reaction chamber, c) sensing chamber and d) its inside view.

off and then the wash cycle was done for the next test solutions. The wash cycle consists of 2.0 M $HNO_3$ (Anedra) followed by ultrapure water. The measurements were performed at the same temperature (24 ± 1°C), so that each of them is equally affected.

*2.1.4. Modification of the QCM-Au sensor surface*

The commercial QCM-Au sensor was purchased from the open QCM store. The sensor is composed of a 6 mm diameter circular gold electrode for the electrical connection, a quartz crystal that oscillates at a frequency of 10 MHz and has a nominal sensitivity of 4.42x10-9 $g\ Hz^{-1}\ cm^{-2}$ [36].

In order to improve the analytical performance of the QCM-Au sensor in the determination of total As, the gold surface was modified by adding nZVI/rGO nanoparticles. These nanoparticles were synthesized by Vinícius de Lima et al. methodology [18]. Briefly, by chemical oxidation and exfoliation of the graphite powder, graphene oxide (GO) was obtained using Hummer's improved method. Then, GO was reduced together with $FeSO_4.7H_2O$ (Aggregate in 1:4 ratio with respect to GO) with an alkaline solution of $NaBH_4$ to finally obtain the nZVI/rGO nanoparticles. The QCM-Au modification was performed by drop-casting methodology as shown in Figure 2. Initially, the QCM-Au was cleaned in an ultrasonic bath with a 1:1 acetone/ethanol mixture for 20 min. Then, 3 $\mu L$ of a 1.0% $(m/v)$ ethanol suspension of nZVI/rGO was added onto the QCM-Au surface and allowed to dry at room temperature. By this way, the modified QCM-Au/nZVI/rGO sensor was obtained [37, 38].

*2.1.5. QCM measurements*

All QCM measurements were performed using an Analog Discovery 2 (Digilent, Inc.) equipped with Waveforms software [39] for impedance analysis. A custom JavaScript code was written in Waveforms software to configure the analysis with a sampling sweep every 10 s and a resolution of 6 Hz. Each of the signals was saved directly to a CSV file.

*2.1.6. Data analysis*

The CSV data file was processed with an Octave script. First, a moving average filter [40] with M (order 9) samples as shown in (3) was employed:

$$y[n] = \frac{1}{M} \sum_{i=0}^{n-1} x[n+i] \tag{3}$$

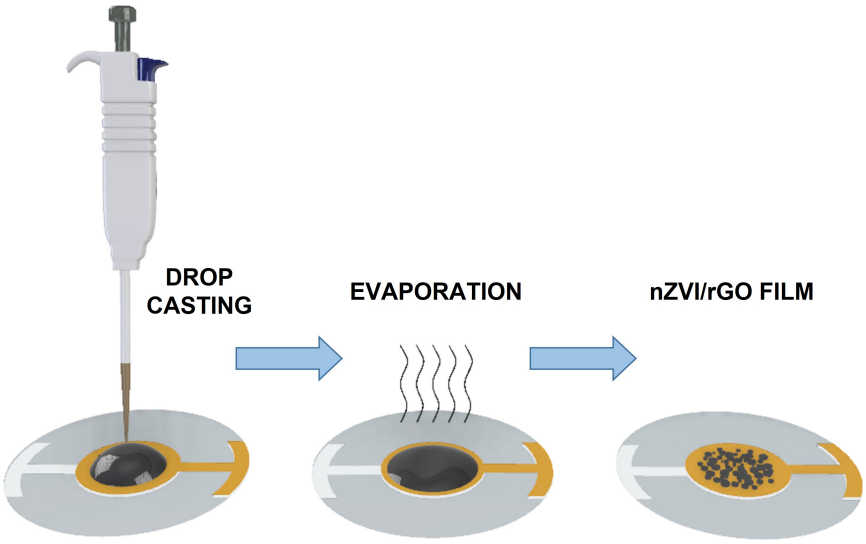


Figure 2: nZVI/rGO coating by drop-casting methodology.

Then, for each sampling sweep, the value of the crystal resonance frequency was determined. This frequency value is directly linked to the maximum admittance value [41].

The smoothed data was plotted using Octave graphics in order to observe the QCM resonance frequency change as a function of measurement time. These signals will be presented in Section 3.1, (see Fig. 3).

### *2.2. Computational details*

In this section, we describe the method used to compute the arsine adsorption on the QCM-Au surface, unmodified and modified. For that, the Density Functional Theory (DFT-U) was used. In particular, the solution to the Kohn-Sham equations with periodic boundary conditions was obtained with the Vienna Ab-initio Simulation Package (VASP) [42, 43, 44].

For this, the Blöch's projector augmented wave (PAW) approach and the periodic plane waves were used in order to describe the core-valence interaction and the electronic states, respectively [45, 46, 47]. Perdew-Burke-Ernzerhof (PBE) within the generalized gradient approximation (GGA-PBE) was used to approximate the exchange-correlation functional. Spin polarized calculations were performed [48].

A $400eV$ kinetic energy cutoff was utilized. Brillouin zone integrations with Γ-centered meshes of 5 x 5 x 5 k-points, and 5 x 5 x 1, were performed

for the bulk and surface structures, respectively. The atoms geometry was fully optimized, reaching a tolerance of $10^{-4}eV$ and $0.05eV/$Å for the energy and the forces, respectively. Moreover, a 15Å and 10Å vacuum regions were utilized in the $Au_{(111)}$ and the nZVI-rGO, respectively, in order to avoid periodic interactions. The Grimme DFT-D2 method was utilized in order to take into account the Van der Waals interaction between pairs [49].

The DFT+U calculations with the $U_{eff}$ Hubbard parameter were performed. In this calculation, DFT is corrected because of the onsite Coulomb interactions enclosed by the Dudarev approximation [50, 51]. The partial occupation of the Fe 3d states in magnetite must be considered in this case. A $U_{eff} = 5eV$ was found to be appropriate.

The equivalent surface formation energy ($E_{SF}$) for the Au(111) surface was calculated using the following equation:

$$E_{\mathrm{SF}} = \frac{E_{\mathrm{Au(111)}} - N_{\mathrm{Au}} E_{\mathrm{Au\text{-}bulk}}}{2S} \tag{4}$$

where $E_{Au(111)}$ is the energy of the Au(111) surface, $N_{Au}$ is the number of Au atoms in the surface, $E_{Au-bulk}$ is the energy of the Au bulk per Au atom and S is the surface area.

The adsorption energies were calculated as follows:

$$E_{\mathrm{ad}} = E_{\mathrm{system+AsH_3}} - E_{\mathrm{AsH_3}} - E_{\mathrm{system}} \tag{5}$$

where $E_{\mathrm{system}}$ is the energy of the substrate system, $E_{\mathrm{AsH_3}}$ is the energy of the arsine and $E_{\mathrm{system+AsH_3}}$ is the energy of the system after adsorption.

Bader analysis was performed in order to obtain the electronic charges on the atoms [52].

The charge density difference analysis of the two adsorbed systems was performed. The charge density difference is calculated according to:

$$\rho(r) = \rho_{\mathrm{system+AsH_3}}(r) - \rho_{\mathrm{AsH_3}}(r) - \rho_{\mathrm{system}}(r) \tag{6}$$

where $\rho_{\mathrm{system+AsH_3}}(r)$, $\rho_{\mathrm{AsH_3}}(r)$ and $\rho_{\mathrm{system}}(r)$ are the total charge on the stable adsorbed configuration, the arsine molecule and the systems, respectively.

## 3. Results and discussion

The ability to detect small frequency changes, due to mass variation by deposition of matter on the surface of the QCM-Au sensor, was combined

with the addition of iron nanoparticles (0) and Reduced Graphene Oxide (rGO). The purpose of this analysis is to evaluate the sensitivity in the determination of total As using the isolated QCM-Au sensor and the modified QCM-Au/nZVI/rGO sensor, employing a Flow-batch system. This study was complemented with a theoretical analysis to justify the experimental results.

### *3.1. Responses from QCM-Au and QCM-Au/nZVI/rGO*

Considering our purpose, responses from the concentrations evaluated of As solutions were obtained using the unmodified (between 5.0-1000.0 $ng\ mL^{-1}$ As) and modified (between 0.01-0.10 $ng\ mL^{-1}$ As) sensor, see Figure 3.

Initially, the adsorption and/or determination of As was tested using the unmodified QCM sensor. Low sensitivity response was obtained for concentrations below 100.0 $ng\ mL^{-1}$ As. Figure 3a shows low frequency changes ($\Delta$f) values corresponding to a low deposition of As on the gold surface of the QCM. Moreover, the $\Delta$f values are within the same range as the resolution of the impedance analyzer, which was set to 6 Hz. Consequently, it is not possible to attribute them to As with sufficient certainty.

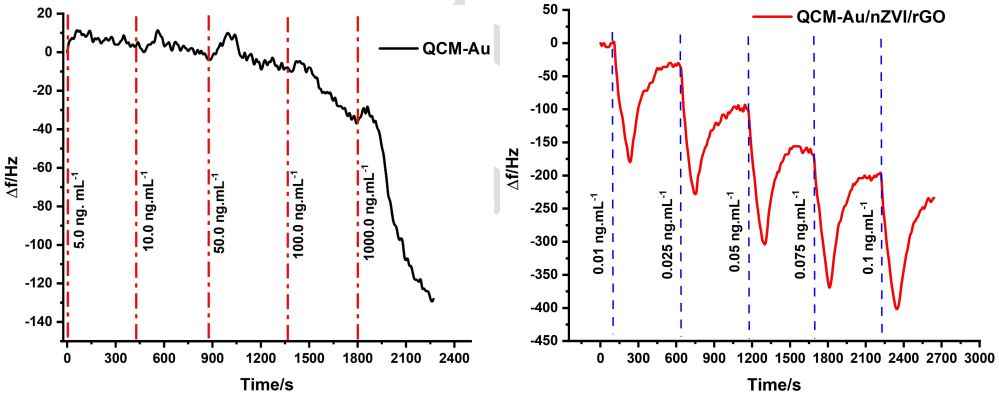


(a) (b)

Figure 3: Frequency changes versus elapsed time versus different As concentrations using a) QCM-Au sensor and b) QCM-Au/nZVI/rGO sensor.

On the other hand, the employ of QCM-Au/nZVI/rGO increases exponentially sensitivity in the As determination. Figure 3b shows that for this case, from As solutions of the order of 0.01 $ng\ mL^{-1}$, the obtained $\Delta$f signals were already distinguishable at that trace level. This shows a big

difference to the results obtained with the sensor without the addition of nanoparticles. This may be due to the strong chemical interaction between As and the surface oxygenated compounds of the nZVI/rGO nanocomposites [53, 54]. This property allowed the small amount of $AsH_3$ that enters the sensing chamber to adhere easily to the surface of the modified sensor and, therefore, to be quantified.

Linear behavior was studied in a concentration range between 0.01-0.10 $ng\ mL^{-1}$ of As. The obtained calibration curve was Y = [2660 ± 110]X + [246 ± 7] [$ng\ mL^{-1}$ As], ($R^2 = 0.995$). The limit of detection (LOD) for the determination of As based on the $3Sb/m$ definition was 0.0062 $ng\ mL^{-1}$ [55]; where Sb is the standard deviation of blank signals for six blank measurements and m, the slope of the calibration.

### *3.2. Reusability of the nZVI/rGO nanoparticles on QCM surface*

The reusability of the sensor was evaluated by conducting 90 consecutive adsorption cycles under the optimized conditions by using 0.05 $ng\ mL^{-1}$ arsenic sample solutions. The arsenic test solutions were detected through the sensor. Afterward, a significant decrease in arsine detection (85–92%) was observed in the following 91-120 cycles. Good reusability was achieved, with coefficients of variation ranged between 4% and 5%. Therefore, the extended use of the nZVI/rGO materials up to 91 cycles in the detection of trace arsenic from water samples is feasible.

### *3.3. Analytical features*

Table 1 shows the comparison of analytical characteristics of the proposed method with respect to other methodologies, also used to determine arsenic in water. It can be seen that our method is more environmentally friendly, since it does not use toxic organic reagents as in the works [56, 35]. Related to sample rate, the above-mentioned determinations present a similar time-dependent sample analysis capacity, with the exception of the work of Anthemidis et al. which is considerably higher. However, the weak points of this work are associated to the high cost of the instrumentation and its great complexity. Regarding the LOD achieved in the presented work, it was better in comparison with the other methodologies, being around 100 times lower than that obtained with SWV and nanomaterials [57]. In contrast to the cited works, the nanomaterials deposited on the surface of the piezoelectric sensor have the ability to be reused for subsequent analyses [18]. Finally, the proposed work presents two remarkable features, an online

extraction/determination step, and in turn, the possibility of miniaturizing or simplifying the system.

| | Anthemidis et al. [58] | Hu et al. [57] | Belen et al. [56] | Vallese et al. [35] | Proposed method |
|---|---|---|---|---|---|
| Detection limit [$\mu g\ L^{-1}$] | 0.06 | 1.19 | 0.07 | 0.03 | 0.0062 |
| Sampling rate [$h^{-1}$] | 41 | ND | 6 | 9 | 7 |
| Reagents | $NaBH_4$, HCl | Buffer phosphate | $NaBH_4$, pyridine, *AgDDTC | $NaBH_4$, pyridine, *AgDDTC | $NaBH_4$, HCl |
| Extraction/ detection | Online | Offline | Online | Online | Online |
| Miniaturization/ simplification | No | Yes | Yes | Yes | Yes |
| Reusability of the surface sensor | - | No | No | No | Yes |
| Instrumentation | Atomic absorption | Electrochemical | Digital microscope | Digital microscope | QCM |

Table 1: Comparative features of different methods for determination of arsenic in water. * AgDDTC: silver diethylditiocarbamate, ND: No declared.

### *3.4. Theoretical calculations of the interaction of $AsH_3$ with the QCM-Au/nZVI/rGO sensor*

The two situations considered previously were analyzed from a theoretical point of view. Initially, the Au(111) surface was modeled to represent the unmodified QCM-Au material (Figure 4c) [59]. We found a surface formation energy of 1.36 $J/m^2$, which is in good agreement with Vitos et al. [60]. These authors calculated a formation energy of 1.28 $J/m^2$, which is a good sign that our surface is correctly modeled. Afterwards, arsine was doped on the Au(111) surface, which resembles the QCM-Au system. Different configurations, orientations and surface sites were tested. The most stable configuration corresponds to an Au top site, with the As atom being closest to the surface, which is shown in Figures 4a-4b.

The other situation present in the experimental setup is the adsorption of the arsine on the nZVI/rGO. So, a model composed of the arsine doped on

the nZVI/rGO structures was studied. A perfect graphene sheet was used to model the rGO. In the case of nZVI, it was modeled as a small cluster of magnetite ($Fe_3O_4$) composed of relaxed (001) layers of $Fe_3O_4$. Since the structure of the nZVI is commonly an iron oxide shell with an iron zero core, in which one of the possible structures is magnetite [61, 13], we proposed this model as a first approach. It has to be mentioned that magnetite is a ferromagnetic material with a cubic inverse spinel structure, where the oxygens form a FCC lattice and the iron atoms occupy the octahedral and tetrahedral interstitial sites [62, 63].

Different orientations and sites were tested for arsine adsorption, finding that the most stable one is the adsorption on an oxygen bridge site, with the As atom pointing towards the surface (Figures 4d-4e).

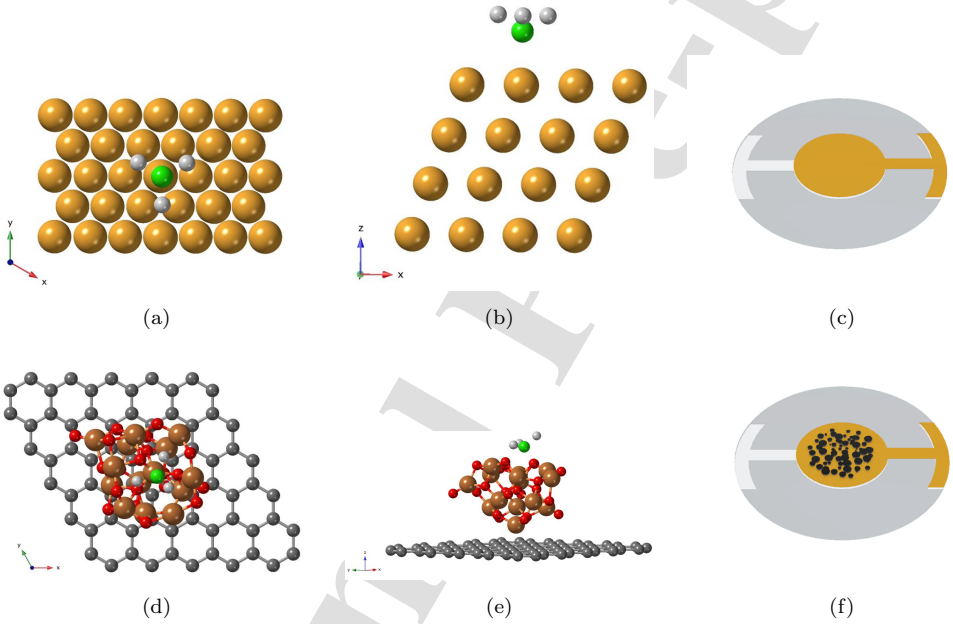


Figure 4: Adsorption of $AsH_3$ on Au(111), seen from (a) the schematic top view, (b) the schematic lateral view and (c) unmodified QCM-Au sensor representation. Adsorption of $AsH_3$ on nZVI/rGO, seen from (d) the schematic top view, (e) the schematic lateral view and (f) modified QCM sensor representation. The light gray, green, yellow, red, brown and grey spheres represent H, As, Au, O, Fe and C species, respectively.

The adsorption energy and the distance found between the arsine and the Au surface were -1.85 $eV$ and 2.52 Å, respectively. The average As-H bonds and H-As-H angles were also calculated, obtaining values of 1.53 Å and 98° respectively. These results indicate favorable and stable adsorption

on the gold surface. The As-H bond values are in good agreement with the results obtained in literature [64], whereas the average angle is 8% higher than the theoretical value of 91° for the isolated arsine molecule, which can be related to the fact that the molecule could be starting to dissociate over the surface.

For the modified sensor modeled system, the total adsorption energy for this site was -2.70 $eV$. The distance between arsine and magnetite was found to be 1.74 Å. Moreover, the average As-H bond and H-As-H angle obtained were 1.52 Å and 110°, respectively. These results indicate a 46% higher stability for the arsine doping on the nZVI/rGO system in comparison with the gold surface, in agreement with the experimental results. Moreover, the distance between arsine and magnetite shortened by 31% and the average angle increased, in comparison to the adsorption on the Au surface. Therefore, these are good indications that the system in Figures 4d-4e is more favorable for the $AsH_3$ adsorption.

The Bader charge analysis of both systems were studied. These show a net atomic charge variation for arsine of 0.3e and 1.2e on Au(111) and nZVI/rGO, respectively, as it can be seen in Table 2. Moreover, the Bader charge of the As atom is in the same tendency as before. Therefore, this is in agreement with the fact that the second system is more favorable for arsine adsorption. In both cases, there is a charge transfer from the arsine to the substrates.

| System | $AsH_3$ charge | As charge | As-nearest system atom BO | As SBO | As-H atoms average BO |
|---|---|---|---|---|---|
| $AsH_3/Au_{(111)}$ | 0.3 | 0.9 | 0.79 | 3.52 | 0.83 |
| $AsH_3/nZVI-rGO$ | 1.2 | 1.6 | 1.17 | 3.74 | 0.74 |

Table 2: Bader charge (e-), bond order (BO) of As with the nearest system atom, sum of bond order (SBO) for As atom and average bond order for As with H atoms.

Charge density difference analysis of both of the systems in discussion were performed. In agreement with the Bader charge analysis, a stronger transference of charge from the arsine molecule to the magnetite is observed (Figure 5). Moreover, charge transfer is more present throughout the magnetite and not localized in one single spot, which again indicates that the nZVI nanoparticles produce a positive effect for the analysis of arsine in comparison with the pure gold surface.

Furthermore, a bond order study was performed to take into account the

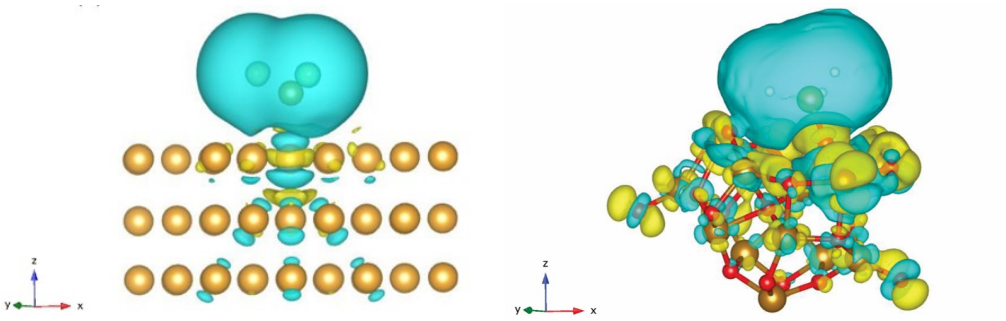

(a) (b)

Figure 5: Isosurface plots at 0.001 e/Å3 for $AsH_3$ adsorbed on (a) the Au(111) surface and (b) the nZVI/rGO system. The yellow and light blue represent electron gain and loss, respectively. The light gray, green, yellow, red and brown spheres represent H, As, Au, O and Fe species, respectively.

strength of the bonding. These results are shown in Table 2. The As bond order is 48% stronger in the case of the $AsH_3$ on nZVI/rGO than on the Au surface, and the Sum of the Bond Order (SBO) of the As atom is 6% higher too. These facts are in agreement with the higher adsorption energy and charge transfer results. The average BO of As with the H atoms shows that in the nZVI/rGO adsorption, the arsine bonds are weaker, in which case the average arsine angle changes more.

The adsorption of the arsine on the sensor-modified system without the inclusion of the nZVI was also evaluated by theoretical calculations. An adsorption energy of -0.20 $eV$ for the arsine, on the last mentioned system was found, which is much lower than the value of -2.70 $eV$ for the arsine adsorption on the second system of nZVI/rGO, indicating that the nZVI inclusion improves significantly the adsorption energy for the removal of As. Moreover, the Bader charge analysis shows a null net atomic charge variation of the arsine in the sensor-modified system without the nZVI, indicating that there is no charge transfer, in contrast to the result of 1.2e of charge transfer obtained for the adsorption of arsine on the nZVI/rGO system. Moreover, the As-H average bond and the H-As-H angle are 1.54 Å and $90^{o}$, respectively. These results show again that the arsine molecule has no relevant changes in comparison to the literature values for the isolated arsine molecule, and therefore shows less change and interaction than in the adsorption of arsine on the nZVI/rGO system. All of these results indicate that the inclusion of the nZVI in these systems is a key aspect for the

adsorption and removal of arsine.

## 4. Conclusions

A QCM-Au sensor with high analytical performance has been designed for the determination of total As by modifying the surface with zero valent iron nanoparticles supported on reduced graphene oxide. Arsine formation was carried out using an automated Flow-batch system where, using small amounts of reagents and control solutions, trace concentrations of total As could be determined. The frequency changes due to arsenic deposition on the QCM-Au/nZVI/rGO sensor showed a high sensitivity (about 100 times larger than the unmodified QCM sensor) with a LOD of 0.0062 $ng\ mL^{-1}$ As, a high precision and reproducibility (s=0.0021 $ng/mL$), and a good linear correlation for a concentration range between 0.010-0.10 $ng\ mL^{-1}$ As. The increase in surface area due to the addition of these nanocomposites together with the oxygen functional groups of their chemical composition have been responsible for this improvement. In turn, DFT calculations indicated that arsine adsorption is preferred on the nZVI/rGO system compared to the smooth Au surface. A distributed charge transfer from $AsH_3$ to the magnetite occurs, which ends up with a positive charge of +1.2e, according to Bader and charge density difference analyses. Furthermore, the nZVI/rGO exhibits stronger atomic bonding compared to the Au(111) surface based on the shorter As-nZVI/rGO bond distances and higher bond order values for this bond. This is in agreement with the theoretical-experimental results mentioned above. Therefore, the system employing a QCM-Au sensor modified with nZVI/rGO is available as a promising application for the determination of arsenic in real samples.

## Founding sources

This research did not receive any specific grant from funding agencies in the public, commercial, or not-for-profit sectors.

## CRediT authorship contribution statement

**Julián Gutiérrez**: Methodology, Software, Validation, Investigation, Visualization. **Yael N. Robein**: Methodology, Validation, Investigation, Visualization. **Julián Juan**: Methodology, Validation, Investigation, Visualization. **Maria S. Di Nezio**: Conceptualization, Software, Supervi-

sion, Writing - review & editing. **Carolina Pistonesi**: Software, Project administration, Funding acquisition, Writing - review & editing. **Estela A. González**: Conceptualization, Project administration, Funding acquisition, Writing - review & editing. **Rodrigo M. Santos**: Conceptualization, Project administration, Funding acquisition, Writing - review & editing. **Marcelo F. Pistonesi**: Conceptualization, Project administration, Funding acquisition, Writing - review & editing.

## Declaration of competing interest

The authors declare that they have no known competing financial interests or personal relationships that could have appeared to influence the work reported in this paper.

## Acknowledgements

Authors acknowledge financial support from Universidad Nacional del Sur (INQUISUR, ICIC, IFISUR). J. Gutiérrez, Y.N. Robein, J. Juan, M.S. Di Nezio, C. Pistonesi, E.A. González and R.M. Santos thanks to Consejo Nacional de Investigaciones Científicas y Técnicas (CONICET, Argentina). M.F. Pistonesi is also grateful to CIC (Comisión de Investigaciones Científicas de la Provincia de Buenos Aires).

## References

[1] L. Sartore, M. Barbaglio, L. Borgese, E. Bontempi, Polymer-grafted qcm chemical sensor and application to heavy metal ions real time detection, Sensors and Actuators B: Chemical 155 (2) (2011) 538–544. doi:10.1016/j.snb.2011.01.003.

[2] D.-M. Li, S.-Q. Li, J.-Y. Huang, Y.-L. Yan, S.-Y. Zhang, X.-H. Tang, J. Fan, S.-R. Zheng, W.-G. Zhang, S.-L. Cai, A recyclable bipyridine-containing covalent organic framework-based qcm sensor for detection of hg(ii) ion in aqueous solution, Journal of Solid State Chemistry 302 (2021) 122421. doi:10.1016/j.jssc.2021.122421.

[3] S. Na Songkhla, T. Nakamoto, Overview of quartz crystal microbalance behavior analysis and measurement, Chemosensors 9 (12) (2021). doi:10.3390/chemosensors9120350.

[4] L. Eddaif, A. Shaban, J. Telegdi, I. Szendro, A piezogravimetric sensor platform for sensitive detection of lead (ii) ions in water based on calix[4]resorcinarene macrocycles: Synthesis, characterization and detection, Arabian Journal of Chemistry 13 (2) (2020) 4448–4461. doi:10.1016/j.arabjc.2019.09.002.

[5] F. Fauzi, A. Rianjanu, I. Santoso, K. Triyana, Gas and humidity sensing with quartz crystal microbalance (qcm) coated with graphene-based materials – a mini review, Sensors and Actuators A: Physical 330 (2021) 112837. doi:10.1016/j.sna.2021.112837.

[6] O. Alev, N. Sarıca, O. Özdemir, L. Çolakerol Arslan, S. Büyükköse, Z. Z. Öztürk, Cu-doped zno nanorods based qcm sensor for hazardous gases, Journal of Alloys and Compounds 826 (2020) 154177. doi:10.1016/j.jallcom.2020.154177.

[7] P. Sun, Y. Chen, M. Yan, T. Tang, Enhancement of qcm detection for heavy metal ions based on tga modified cdte nanospheres, Journal of Inorganic and Organometallic Polymers and Materials 30 (2) (2020) 525–531. doi:10.1007/s10904-019-01212-1.

[8] Arsenic, world health organization, accessed: 2023-08-23 (2022).
URL https://www.who.int/news-room/fact-sheets/detail/arsenic

[9] S. Joshi, M. Sharma, A. Kumari, S. Shrestha, B. Shrestha, Arsenic removal from water by adsorption onto iron oxide/nano-porous carbon magnetic composite, Applied Sciences (Switzerland) 9 (18) (2019). doi:10.3390/app9183732.

[10] S. O. Adio, M. H. Omar, M. Asif, T. A. Saleh, Arsenic and selenium removal from water using biosynthesized nanoscale zero-valent iron: A factorial design analysis, Process Safety and Environmental Protection 107 (2017) 518 – 527. doi:10.1016/j.psep.2017.03.004.

[11] Z. Wen, J. Lu, Y. Zhang, G. Cheng, S. Huang, J. Chen, R. Xu, Y. an Ming, Y. Wang, R. Chen, Facile inverse micelle fabrication of magnetic ordered mesoporous iron cerium bimetal oxides with excellent performance for arsenic removal from water, Journal of Hazardous Materials 383 (2020) 121172. doi:10.1016/j.jhazmat.2019.121172.

[12] J. Tucek, R. Prucek, J. Kolarik, G. Zoppellaro, M. Petr, J. Filip, V. K. Sharma, R. Zboril, Zero-valent iron nanoparticles reduce arsenites and arsenates to as (0) firmly embedded in core–shell superstructure: Challenging strategy of arsenic treatment under anoxic conditions, ACS Sustainable Chemistry & Engineering 5 (4) (2017) 3027–3038. doi:10.1021/acssuschemeng.6b02698.

[13] W. Yan, M. A. V. Ramos, B. E. Koel, W.-x. Zhang, As(iii) sequestration by iron nanoparticles: Study of solid-phase redox transformations with x-ray photoelectron spectroscopy, The Journal of Physical Chemistry C 116 (9) (2012) 5303–5311. doi:10.1021/jp208600n.

[14] Y. Sun, C. Ding, W. Cheng, X. Wang, Simultaneous adsorption and reduction of u (vi) on reduced graphene oxide-supported nanoscale zerovalent iron, Journal of Hazardous Materials 280 (2014) 399–408. doi:10.1016/j.jhazmat.2014.08.023.

[15] L. Ren, J. Dong, Z. Chi, H. Huang, Reduced graphene oxide-nano zero value iron (rgo-nzvi) micro-electrolysis accelerating cr (vi) removal in aquifer, Journal of environmental sciences 73 (2018) 96–106. doi:10.1016/j.jes.2018.01.018.

[16] S. Khoshro, N. S. Mirbagheri, S. Sabbaghi, Removal of nitrate from aqueous solution using nano zerovalent iron-reduced graphene oxide composite: optimization of parameters, Water and Environment Journal 34 (2020) 608–621. doi:10.1111/wej.12564.

[17] W. Liu, J. Bai, Z. Chi, L. Ren, J. Dong, An in-situ reactive zone with xanthan gum modified reduced graphene oxide supported nanoscale zero-valent iron (xg-nzvi/rgo) for remediation of cr (vi)-polluted aquifer: Dynamic evolutions of cr (vi) and environmental variables, Journal of Environmental Chemical Engineering 9 (1) (2021) 104987. doi:10.1016/j.jece.2020.104987.

[18] C. Vinícius de Lima, J. Juan, R. Faccio, E. A. González, C. Pistonesi, M. F. Pistonesi, J. S. Rebouças, Arsenic adsorption on nanoscale zerovalent iron im-

mobilized on reduced graphene oxide (nzvi/rgo): Experimental and theoretical approaches, The Journal of Physical Chemistry C 126 (46) (2022) 19916–19925. doi:10.1021/acs.jpcc.2c06206.

[19] C. Wang, H. Luo, Z. Zhang, Y. Wu, J. Zhang, S. Chen, Removal of as(iii) and as(v) from aqueous solutions using nanoscale zero valent iron-reduced graphite oxide modified composites, Journal of Hazardous Materials 268 (2014) 124–131. doi:10.1016/j.jhazmat.2014.01.009.

[20] S. Momeni, M. Farrokhnia, S. Karimi, I. Nabipour, Copper hydroxide nanostructure-modified carbon ionic liquid electrode as an efficient voltammetric sensor for detection of metformin: a theoretical and experimental study, Journal of the Iranian Chemical Society 13 (6) (2016) 1027–1035.

[21] E. C. Mattson, K. Pande, M. Unger, S. Cui, G. Lu, M. Gajdardziska-Josifovska, M. Weinert, J. Chen, C. J. Hirschmugl, Exploring adsorption and reactivity of nh3 on reduced graphene oxide, The Journal of Physical Chemistry C 117 (20) (2013) 10698–10707. doi:10.1021/jp3122853.

[22] J.-E. Jung, S. Liguori, A. D. Jew, G. E. B. Jr., J. Wilcox, Theoretical and experimental investigations of mercury adsorption on hematite surfaces, Journal of the Air & Waste Management Association 68 (1) (2018) 39–53. doi:10.1080/10962247.2017.1362364.

[23] A. Arularasan, A. Kumar, Dft investigation of bi (100) and au (111) for heavy metal ion adsorption and selective comparison for water quality sensing electrodes, International journal of simulation: systems, science & technology (2019). doi:10.5013/IJSSST.A.19.06.59.

[24] L. L. Alfonso Tobón, S. Fuente, M. M. Branda, Electronic and magnetic properties of the adsorption of as harmful species on zero-valent fe surfaces, clusters and nanoparticules, Applied Surface Science 465 (2019) 715–723. doi:10.1016/j.apsusc.2018.09.199.

[25] A. F. Hassan, R. Hrdina, Enhanced removal of arsenic from aqueous medium by modified silica nanospheres: Kinetic and thermodynamic studies, Arabian Journal for Science and Engineering 47 (1) (2022) 281–293.

[26] L. L. Alfonso Tobón, M. M. Branda, Predicting the adsorption capacity of iron nanoparticles with metallic impurities (cu, ni and pd) for arsenic removal: a DFT study, Adsorption 26 (1) (2020) 127–139.

[27] D. Cortes-Arriagada, A. Mella, Performance of doped graphene nanoadsorbents with first-row transition metals (sczn) for the adsorption of water-soluble trivalent arsenicals: A dft study, Journal of Molecular Liquids 294 (2019) 111665. doi:10.1016/j.molliq.2019.111665.

[28] M. Srivastava, A. Srivastava, S. Pandey, Suitability of graphene monolayer as sensor for carcinogenic heavy metals in water: A dft investigation, Applied Surface Science 517 (2020) 146021. doi:10.1016/j.apsusc.2020.146021.

[29] K. Li, H. Yang, X. Yuan, M. Zhang, Recent developments of heavy metals detection in traditional chinese medicine by atomic spectrometry, Microchemical Journal 160 (2021) 105726. doi:10.1016/j.microc.2020.105726.

[30] V. M. Shchukin, E. S. Zhigilei, A. A. Erina, Y. N. Shvetsova, N. E. Kuz'mina, A. I. Luttseva, Validation of an ICP-MS method for the determination of mercury, lead, cadmium, and arsenic in medicinal plants and related drug preparations, Pharma-

ceutical Chemistry Journal 54 (9) (2020) 968–976.

[31] J. Ran, D.-J. Wang, C. Wang, L.-J. Bo, J.-C. Zheng, L.-P. Yao, Comparison of soil heavy metals determined by aas/afs and portable x-ray fluorescence analysis, Guang Pu Xue Yu Guang Pu Fen Xi/Spectroscopy and Spectral Analysis 34 (11) (2014) 3113 – 3118. doi:10.3964/j.issn.1000-0593(2014)11-3113-06.

[32] B. Bansod, T. Kumar, R. Thakur, S. Rana, I. Singh, A review on various electrochemical techniques for heavy metal ions detection with different sensing platforms, Biosensors and Bioelectronics 94 (2017) 443–455. doi:10.1016/j.bios.2017.03.031.

[33] J. Gutiérrez, J. P. Mochen, G. Eggly, M. Pistonesi, R. Santos, Open source automated flow analysis instrument for detecting arsenic in water, HardwareX 11 (2022) e00284. doi:10.1016/j.ohx.2022.e00284.

[34] I. Hagarová, M. Bujdos, L. Canecka, P. Matúš, Reliability of arsenic speciation analysis in four reaction media by hydride generation atomic absorption spectrometry, Fresenius Environmental Bulletin 20 (2011) 2927–2931.

[35] F. D. Vallese, F. Belén, P. V. Messina, A. de Araújo Gomes, M. F. Pistonesi, Exploiting a gradient kinetics and color histogram in a single picture to second order digital imaging data acquisition with mcr-als for the arsenic quantification in water, Sensors and Actuators B: Chemical 342 (2021) 130079. doi:10.1016/j.snb.2021.130079.

[36] openQCM, The open-source quartz crystal microbalance (qcm), last accessed 14 May 2023 (2023).
URL `https://store.openqcm.com/10-MHZ-QUARTZ-SENSORS-BOX-10-PIECES/`

[37] Z. Wu, X. Chen, S. Zhu, Z. Zhou, Y. Yao, W. Quan, B. Liu, Enhanced sensitivity of ammonia sensor using graphene/polyaniline nanocomposite, Sensors and Actuators B: Chemical 178 (2013) 485–493. doi:10.1016/j.snb.2013.01.014.

[38] P. Qi, Z. Wang, R. Wang, Y. Xu, T. Zhang, Studies on qcm-type no2 gas sensor based on graphene composites at room temperature, Chemical Research in Chinese Universities 32 (6) (2016) 924–928. doi:10.1007/s40242-016-6129-z.

[39] Digilent, Waveforms reference manual, last accessed 1 June 2023 (2023).
URL `https://digilent.com/reference/software/waveforms/waveforms-3/reference-manual`

[40] S. W. Smith, Chapter 15 - moving average filters, in: S. W. Smith (Ed.), Digital Signal Processing, Newnes, Boston, 2003, pp. 277–284. doi:10.1016/B978-0-7506-7444-7/50052-2.

[41] S. J. Martin, V. E. Granstaff, G. C. Frye, Characterization of a quartz crystal microbalance with simultaneous mass and liquid loading, Analytical Chemistry 63 (20) (1991) 2272–2281. doi:10.1021/ac00020a015.

[42] P. Hohenberg, W. Kohn, Inhomogeneous electron gas, Phys. Rev. 136 (1964) B864–B871. doi:10.1103/PhysRev.136.B864.

[43] W. Kohn, L. J. Sham, Self-consistent equations including exchange and correlation effects, Phys. Rev. 140 (1965) A1133–A1138. doi:10.1103/PhysRev.140.A1133.

[44] G. Kresse, D. Joubert, From ultrasoft pseudopotentials to the projector augmented-wave method, Phys. Rev. B 59 (1999) 1758–1775. doi:10.1103/PhysRevB.59.1758.

[45] G. Kresse, J. Furthmüller, Efficiency of ab-initio total energy calculations for metals and semiconductors using a plane-wave basis set, Computational Materials Science 6 (1) (1996) 15–50. doi:10.1016/0927-0256(96)00008-0.

[46] G. Kresse, J. Furthmüller, Efficient iterative schemes for ab initio total-energy calculations using a plane-wave basis set, Phys. Rev. B 54 (1996) 11169–11186.

doi:10.1103/PhysRevB.54.11169.
[47] P. E. Blöchl, Projector augmented-wave method, Phys. Rev. B 50 (1994) 17953–17979. doi:10.1103/PhysRevB.50.17953.
[48] J. P. Perdew, K. Burke, M. Ernzerhof, Generalized gradient approximation made simple, Phys. Rev. Lett. 77 (1996) 3865–3868. doi:10.1103/PhysRevLett.77.3865.
[49] S. Grimme, Semiempirical gga-type density functional constructed with a long-range dispersion correction, Journal of Computational Chemistry 27 (15) (2006) 1787–1799. doi:10.1002/jcc.20495.
[50] S. L. Dudarev, G. A. Botton, S. Y. Savrasov, C. J. Humphreys, A. P. Sutton, Electron-energy-loss spectra and the structural stability of nickel oxide: An lsda+u study, Phys. Rev. B 57 (1998) 1505–1509. doi:10.1103/PhysRevB.57.1505.
[51] S. L. Dudarev, G. A. Botton, S. Y. Savrasov, Z. Szotek, W. M. Temmerman, A. P. Sutton, Electronic structure and elastic properties of strongly correlated metal oxides from first principles: Lsda + u, sic-lsda and eels study of uo2 and nio, physica status solidi (a) 166 (1) (1998) 429–443. doi:10.1002/(SICI)1521-396X(199803)166:1¡429::AID-PSSA429¿3.0.CO;2-F.
[52] W. Tang, E. Sanville, G. Henkelman, A grid-based bader analysis algorithm without lattice bias, Journal of Physics: Condensed Matter 21 (8) (2009) 084204. doi:10.1088/0953-8984/21/8/084204.
[53] J. Ferro Falla, Síntesis verde de nanopartículas de hierro cero valente para la remoción de cadmio, cromo y arsénico en solución, Master's thesis, Universidad de los Andes, Bogotá, Colombia (2020).
[54] Q. Rodríguez Melendez, Síntesis de óxido de grafeno para la remoción de arsénico en agua, Master's thesis, Centro de Investigación y de Estudios Avanzados del Instituto Politécnico Nacional, Saltillo, Mexico (2018).
[55] M. Al-Tameemi, S. Arif, A. Campiglia, W. Wilson, S. Wise, Photoluminescence spectroscopy of anthrathiophenes and benzonaphthothiophenes in shpol'skii matrixes, Talanta 194 (2019) 930–940. doi:10.1016/j.talanta.2018.10.044.
[56] F. Belén, F. D. Vallese, L. G. Leist, M. F. Ferrão, A. de Araújo Gomes, M. F. Pistonesi, Computer-vision based second-order (kinetic-color) data generation: arsenic quantitation in natural waters, Microchemical Journal 157 (2020) 104916. doi:10.1016/j.microc.2020.104916.
[57] H. Hu, W. Lu, X. Liu, F. Meng, J. Zhu, A high-response electrochemical as(iii) sensor using fe3o4–rgo nanocomposite materials, Chemosensors 9 (6) (2021). doi:10.3390/chemosensors9060150.
[58] A. N. Anthemidis, G. A. Zachariadis, J. A. Stratis, Determination of arsenic(iii) and total inorganic arsenic in water samples using an on-line sequential insertion system and hydride generation atomic absorption spectrometry, Analytica Chimica Acta 547 (2) (2005) 237–242. doi:10.1016/j.aca.2005.05.039.
[59] M. Mura, A. Gulans, T. Thonhauser, L. Kantorovich, Role of van der waals interaction in forming molecule-metal junctions: flat organic molecules on the au(111) surface, Phys. Chem. Chem. Phys. 12 (2010) 4759–4767. doi:10.1039/B920121A.
[60] L. Vitos, A. Ruban, H. Skriver, J. Kollár, The surface energy of metals, Surface Science 411 (1) (1998) 186–202. doi:10.1016/S0039-6028(98)00363-X.
[61] W. Yan, R. Vasić, A. I. Frenkel, B. E. Koel, Intraparticle reduction of arsenite (as(iii)) by nanoscale zerovalent iron (nzvi) investigated with in situ x-ray absorp-

tion spectroscopy, Environmental Science & Technology 46 (13) (2012) 7018–7026. doi:10.1021/es2039695.

[62] M. E. Fleet, The structure of magnetite, Acta Crystallographica Section B 37 (4) (1981) 917–920. doi:10.1107/S0567740881004597.

[63] M. E. Fleet, The structure of magnetite: Symmetry of cubic spinels, Journal of Solid State Chemistry 62 (1) (1986) 75–82. doi:10.1016/0022-4596(86)90218-5.

[64] H. H. Nielsen, The molecular structure of arsine, The Journal of Chemical Physics 20 (12) (1952) 1955–1956. doi:10.1063/1.1700347.

## Research Highlights

- A sensor based on a gold Quartz Crystal Microbalance (QCM) modified with nanoscale zero-valent iron nanoparticles (nZVI) anchored to reduced graphene oxide (rGO) was developed.
- Density Functional Theory (DFT) methodology was used employing arsine adsorption on magnetite nanoparticles supported on Graphene and also on Au as models.
- The gold surface QCM modification with nZVI/rGO improved the sensitivity in total As determination.
- This theoretical-experimental research allows to acquire knowledge of the interaction of Au/nZVI/rGO with As and confirms the experimental results.

**Julián Gutiérrez** received his Electronic Engineering degree in 2021 and he is currently doing his Ph.D in Engineering at Universidad Nacional del Sur, Bahía Blanca, Argentina, with a fellowship from Argentine Research Council (CONICET). His research interest is the development of flow-batch systems for the determination of arsenic in water samples. He is a University Teaching Assistant at the Universidad Nacional del Sur.

**Yael N. Robein** studied chemistry and received his B.S. degree in 2018 and he is currently doing his Ph.D in chemistry at Universidad Nacional del Sur, Bahía Blanca, Argentina, with a fellowship from Argentine Research Council (CONICET). His research interest is the develop voltammetric sensors using Cdots or hybrid silver/carbon nanoparticles (Ag@Cdots) to determine possible contaminants in bee products. Also, He carry out a study of theoretical models (quantum chemistry) implemented to evaluate the interactions between carbon and silver atoms in order to identify the interactions between carbon and silver atoms in order to identify the participation of the carbon nanostructure as a blocking agent on the surface of Ag@Cdots. He is a University Teaching Assistant at the Universidad Nacional del Sur.

**Julián Juan** obtained his PhD. in Physics (2023) from the Universidad Nacional del Sur (UNS) at Bahía Blanca, Argentina. He is a postdoc fellow at Consejo Nacional de Investigaciones Científicas y Técnicas (CONICET). He is a Chief Professor's Assistant at the Universidad Nacional del Sur of Elements of Thermodynamics and Solid State Physics. His research areas are focused on theoretical simulation of energy related materials and computational surface science.

**María S. Di Nezio** obtained her Mg. in chemistry (1996) and PhD in chemistry (2003) from the Universidad Nacional del Sur (UNS) at Bahía Blanca, Argentina and researcher at Instituto de Química del Sur (INQUISUR (UNS-CONICET). She is a Pofessor of analytical chemistry at the Universidad Nacional del Sur. Her main areas of interest focus on the development of automated analytical methods associated with spectroscopy and electroanalytical techniques for the determination of different analytes in food samples.

**Carolina Pistonesi** obtained her PhD. in Science and Technology of Materials (2002) from the Universidad Nacional del Sur (UNS) at Bahía Blanca, Argentina. She is a researcher at Consejo Nacional de Investigaciones Científicas y Técnicas (CONICET). She is a Professor of Physics I at the Universidad Nacional del Sur. Her research areas are focused on the theoretical modeling of surface and 3D materials for catalytic purposes.

**Estela A. González** obtained her PhD. in Science and Technology of Materials (2006) from the Universidad Nacional del Sur (UNS) at Bahía Blanca, Argentina. She is a researcher at Consejo Nacional de Investigaciones Científicas y Técnicas (CONICET). She is a Professor of Physics I at the Universidad Nacional del Sur. Her research areas are focused on computational surface science and the development of models of catalytic surfaces, interfaces and 3D solids.

**Rodrigo M. Santos** received the degree in engineering and the Ph.D. degree from the Department of Electrical and Computers, Universidad Nacional del Sur (UNS). He is currently an Adjunct Professor and a Researcher with UNS and CONICET, Argentina. His research interests are in the field of real-time systems, embedded systems,and collaborative systems. He has been the President of the Center of Latin American for Studies in Informatics and the Vice Chair of the IFIP WG 6.9 Communications for Developing Countries.

**Marcelo F. Pistonesi** obtained his PhD in chemistry (2001) from the Universidad Nacional del Sur (UNS) at Bahía Blanca, Argentina and researcher at Comisión de Investigaciones Científicas de la provincia de Buenos Aires (CIC).He is a professor of analytical chemistry at the Universidad Nacional del Sur. His areas of research are focused on the environment, automation and electronics.

**Declaration of interests**

☒ The authors declare that they have no known competing financial interests or personal relationships that could have appeared to influence the work reported in this paper.

☐ The authors declare the following financial interests/personal relationships which may be considered as potential competing interests: